AQUA
Water Infrastructure, Ecosystems and Society

IWA PUBLISHING

 AQUA — Water Infrastructure, Ecosystems and Society Vol 71 No 8, 938 doi: 10.2166/aqua.2022.070

Runoff estimation using digital image processing for residential areas

Pramod Soni [a,*], Hemanta Medhi[b], Anitya Sagar[a], Pulkit Garg[a], Abhay Singh[a] and Umesh Karna[a]

[a] Department of Civil Engineering, Motilal Nehru National Institute of Technology, Prayagraj, Uttar Pradesh 211004, India
[b] Department of Civil Engineering, Tezpur University, Tezpur, Assam 784028, India
*Corresponding author. E-mail: pramod@mnnit.ac.in

PS, 0000-0001-8700-0238

ABSTRACT

With the burgeoning population worldwide, the demand for freshwater supply is increasing, mostly in urban areas, due to the influx of people for better livelihood. To mitigate this burden of freshwater demand and build a sustainable water management system, harvesting rainwater during the rainfall season is a viable option. Runoff estimation studies in the past are time-intensive as parameter estimation for an area is complex by the conventional method. In this study, the Motilal Nehru National Institute of Technology (MNNIT), Allahabad campus was selected as a pilot project to assess a methodology that uses Google Earth images for obtaining the runoff coefficients. This method is easy and consumes less time in runoff estimation. This was compared with the conventional method. Using the conventional method (Arc-GIS), the equivalent runoff coefficients for these catchments were found to be 0.2780, 0.3553, and 0.4111, respectively. The range of error (compared to the traditional method) in runoff obtained from the proposed method with a default k value (0.8) was found to be 8.16–13.55%, with an average value of 9.91%. However, with a slightly modified value of k (0.9), the errors were significantly reduced to 1.94–3.32%, with an average of 2.15%.

Key words: digital image processing, GIS, rainwater harvesting, runoff, water conservation

HIGHLIGHTS

- A novel method to estimate runoff for a residential catchment.
- Fast and accurate method as compared to the traditional method.

GRAPHICAL ABSTRACT

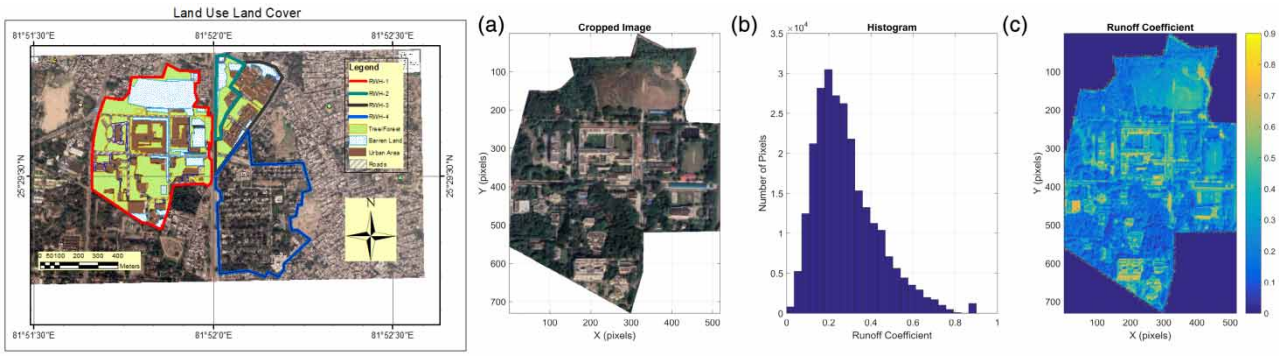

1. INTRODUCTION

Water supply–demand has increased multiple times in the last decade and is expected to increase to 55% by 2050 (Wang *et al.* 2013; Haque *et al.* 2016). This demand is mainly due to the exponential growth of the population and the rapid expansion of and development of urban areas and industries. Moreover, the variability of rainfall in the spatio-temporal direction due to climate change has complicated the situation. Severe water shortages have been predicted by 2050 if no measures are taken to

find new water supply sources (IFPRI 2012). Thus, there is an urgent need for water conservation to cater to the need in these changing times.

Studies of rainfall trend analysis have shown a decreasing trend in various cities worldwide (Amanatidis *et al.* 1993; Jain & Kumar 2012; Zhou *et al.* 2017). Thus, a continuation of this decreasing trend scenario will affect the required availability of freshwater, especially during the non-rainy seasons. Due to urbanization, a significant part of the land cover is transformed into imperviousness (Lindh 1983). Thus, during the rainy season in urban areas, infiltration is low due to a lack of pervious surface, and most of the rainfall flows as surface runoff. The higher surface runoff may cause flood situations where the intensity is high (Hafizi Md Lani *et al.* 2018). Also, the frequency of groundwater recharge becomes low due to urbanization (Foster 1999) which may cause scarcity of the available groundwater. Overexploitation of the groundwater reserves and studies have shown that nations' social and economic growth will be affected due to decreased groundwater availability (Kemper 2004; Garg & Hassan 2007).

Several studies have shown an inverse relationship between rainfall and temperature (Kothyari & Singh 1996; Sharma & Babel 2014; Issahaku *et al.* 2016). Also, an increase in the mean temperature on a global scale is reported by Parker *et al.* (2000). This increase in temperature is attributed to global warming; thus, a decrease in rainfall may be expected. Hence, proper planning and management of the available water resources should be carefully studied to negate any detrimental effects in the future. Also, rainwater harvesting (RWH) methods in such changing environment is a sustainable method to tackle water shortcomings in the future.

The rainwater interacts with the physical characteristics of the basin such that a part is infiltrated depending on the permeability of the surface, and the other part flows as the overland flow. The overland flow can be stored using a RWH system, which otherwise would flow out of the basin (Abdulla & Al-Shareef 2009). The RWH system has been successfully used in various countries to cater to the population's demands (Handia *et al.* 2003). Studies have also shown that the RWH system has been effectively used for agriculture (Falkenmark & Stockholm International Water Institute 2001). In an RWH system, the overland flow runoff can be trapped and stored. However, RWH is not limited to runoff storage alone; in residential areas, the rain that falls on the roof can also be collected. The RWH system helps decrease the dependency on the groundwater and reduce flood risks (Eckart *et al.* 2018; Qi *et al.* 2019; Huang *et al.* 2021).

Studies have shown the RWH system to be cost-efficient and more profitable if implemented on a large scale (Tam *et al.* 2010). Studies regarding RWH conducted in the water-scarce regions in Malaysia pointed to economic, social, and technical challenges. However, it was concluded to be a potential water resources alternative for the region (Lee *et al.* 2016). Other studies also suggest the RWH system as an efficient alternative for reducing the dependencies on fresh water in water-scarce regions (Sample & Liu 2014; Thomas *et al.* 2014; Morales-Pinzón *et al.* 2015). Haque *et al.* (2016) conducted a study on the impacts of climate change on RWH by selecting five locations in Australia. They concluded that the dry season affects the RWH system more than the wet season. Ward *et al.* (2012) studied the performance of a large-building RWH system that showed an average water-saving efficiency of 87% in 8 months. The findings show the significant potential in the savings of water and cost. In Jordan, rooftop RWH system studies by Abdulla & Al-Shareef (2009) showed considerable water saving; however, bacteriological parameters exceeded the limits required for potable water. The water from the RWH system can be used for various non-potable purposes. However, some studies showed that it could be treated so that it can be supplied for drinking and domestic purposes as well (Hartigan 2009; Helmreich & Horn 2009; Zhou *et al.* 2010; Al Qudah *et al.* 2012; Qi *et al.* 2019; Huang *et al.* 2021).

The RWH system studies show great potential in newly developed urban areas (Zabidi *et al.* 2020), thus drawing the interest of many in recent years (Farahbakhsh *et al.* 2009; Belmeziti *et al.* 2014; Vieira *et al.* 2014; Fonseca *et al.* 2017). Research studies have used the SCS-CN (Soil Conservation Service-Curve Number) method to estimate the runoff (Al-Ghobari & Dewidar 2021). In this method, the coefficient, CN, depends on factors like the soil type, land use, land cover, and antecedent soil moisture content. The rational formula is also widely used to compute the runoff for a catchment with known runoff coefficients based on the land use and land cover (LULC) (Biswas & Mandal 2014). Remote sensing and GIS (Geographic Information System) techniques are widely applied in urban environmental analysis for roof surface runoff estimation (Radzali *et al.* 2018; Norman *et al.* 2019) and to identify impervious surfaces and RWH sites (Forkuo 2013; Gaikwad 2015; Mahmoud & Alazba 2015; Ammar *et al.* 2016).

There have been very few studies that have used Google Satellite images for estimation of LULC and runoff coefficients. Medina *et al.* (2012) used high-resolution satellite imagery data from Google Maps in an automated fashion based on the fuzzy set classification to extract the runoff coefficients from satellite images and found promising results. Aher *et al.*

(2014) applied the K-means clustering algorithm and textural parameters based on the gray-level co-occurrence matrix (GLCM) to classify the Google Earth images into land cover and land use sectors. They found that the K-means algorithm works well for classifying satellite images due to its excellent accuracy. Aung & Thant (2019) also applied the K-means clustering algorithm to classify Google Satellite images into three general classes: (1) building, (2) vegetation, and (3) road. Ekbote *et al*. (2017) used a correlation of the template image with the main image employing image normalized cross-correlation to estimate the green spots (tree) area.

The traditional method of computing the runoff coefficient is time-intensive as the LULC over the catchment is different and thus have different runoff coefficients. This process, if done manually, can make the computation even more complex. Thus, in this study, a framework is proposed to estimate the parameters using digital image processing techniques with the help of Google Satellite images.

The present study proposes a simple and novel method to estimate the runoff generation capacity of a limited area using Google Satellite images. It can be used to quickly and efficiently estimate the runoff from the residential areas and then use it to design RWH systems.

2. STUDY AREA AND DATA USED

The residential and academic campus of the Motilal Nehru National Institute of Technology (MNNIT), Allahabad, a premier educational institute in Prayagraj, is considered as the study area for this research work (Figure 1). Prayagraj is located roughly between 8 °N and 37 °N latitude with tropical climatic conditions at an elevation of about over 90 m above sea level. As per the 2011 census report, the total population of the district is 1,112,544 in the 82 km^2 area. The calendar year can be divided into the following four seasons: winter (January and February) having low temperatures, low humidity and clear skies; pre-monsoon (March–May) having high temperatures with hot dry winds; monsoon (June–September) with heavy rainfall all over the country; and post-monsoon (October–December), which is a transition period from monsoon to winter. During the monsoon season, rain from the Bay of Bengal or the Arabian Sea branches of the southwest monsoon supplies the city with most of its annual rainfall.

The MNNIT campus is cantered at 25.4920 °N, 81.8639 °E and houses approximately 6,000 residents. The campus residents are mostly dependent on the groundwater which is recharged during the monsoon season.

For the purpose of designing a RWH system for a small residential area, the watershed cannot be defined by the natural drainage, but by the available drainage network. The drainage network of the campus was obtained from the civil maintenance office, MNNIT, Allahabad. Based on the available drainage network of the institute, the four catchments are defined as shown in Figure 1.

3. METHODOLOGY

To design a RWH for any given catchment area, it is a must to compute the total runoff generated from the catchment. The most widely used method of runoff estimation is the Rational Method, which can be used for areas less than 50 acres. According to this method, the expression for the runoff produced from a watershed:

$$Q = CiA$$

Here, C is the runoff coefficient, i is the intensity of rainfall, and A is the area of the watershed. The runoff coefficient for any area is the ratio of the volume of water that runs off a surface to the volume of rainfall that falls on the surface. It accounts for the losses such as infiltration, evaporation, etc. and ranges between 0 and 1. If $C = \{C_1,\ C_2,\ \ldots,\ C_n\}$ are the runoff coefficients for the respective areas, $A = \{A_1,\ A_2,\ \ldots,\ A_n\}$ in a catchment having n number of land types, then the equivalent runoff coefficient (C_{eq}) for the area is given by:

$$C_{eq} = \frac{\sum_{i=1}^{n} C_i A_i}{\sum_{i=1}^{n} A_i} \tag{1}$$

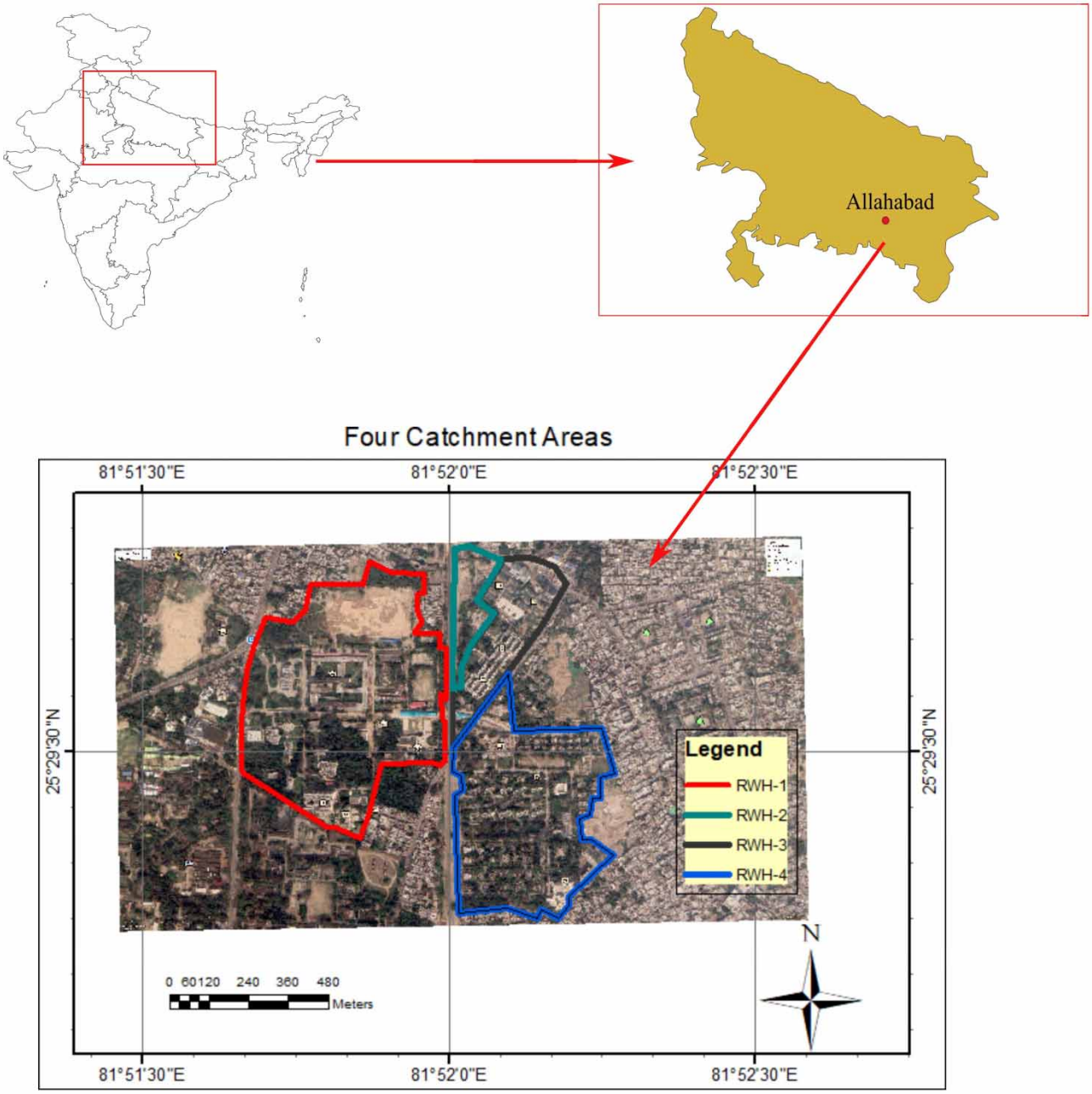

Figure 1 | Study area: MNNIT, Allahabad campus. Please refer to the online version of this paper to see this figure in colour: http://dx.doi.org/10.2166/aqua.2022.070.

In the traditional method for estimating the total runoff, the entire map is georeferenced, the area of each individual land use type is estimated, and finally, the equivalent runoff coefficient is computed using Equation (1). However, in the proposed method, we can estimate the equivalent runoff coefficient by processing the Google Earth Satellite image based on the colour of each pixel. The satellite imagery of the extent of the MNNIT campus was obtained from Google Earth and then georeferenced using six ground control points. Based on the drainage network of the MNNIT campus and the satellite image, the campus was divided into four catchments and suitable locations of the RWH system were identified (Figure 1). In the absence of an existing (only proposed available) drainage network of RWH-4, the study was carried out for three catchments only (RWH-1, RWH-2, and RWH-3). The runoff coefficients were computed using Google Satellite imaginary with the help of MATLAB, which were then used to estimate the runoff volume. The digital number of each pixel of the satellite was analysed

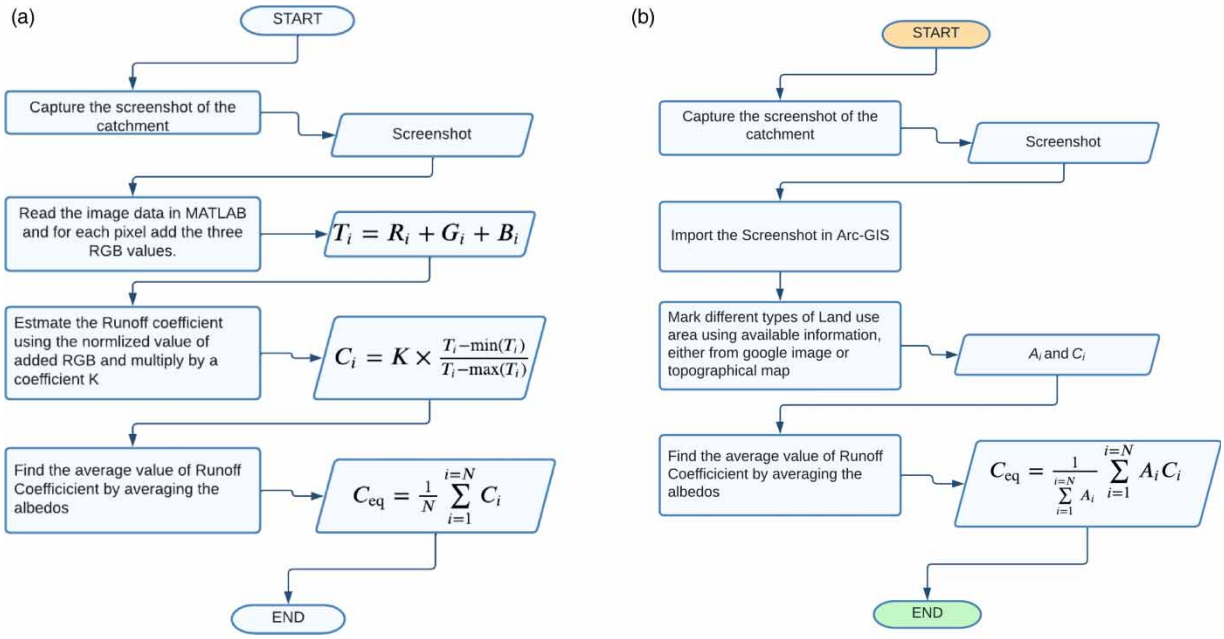

Figure 2 | Flow chart for runoff coefficient estimation: (a) image processing and (b) conventional (Arc-GIS processing).

and then attributed to the physical characteristics of the catchment. The image processing methodology is explained in Figure 2(a)

- The cropped image of the catchment (the outer boundary of the catchment should be completely white).
- Read the image data in MATLAB (or any suitable image processing software). For each pixel, add all the three R-G-B colour values to a variable T_i. The maximum value of T_i would be 765 (255+255+255) for the entirely white area that is outside the catchment boundary and 0 for entirely dark (black) areas. These entirely white areas would be discarded from further analysis, as they are outside the marked catchment.
- Compute the runoff coefficient for each pixel by using the following formula.

$$C_i = K \times \frac{T_i - \min(T_i)}{\max(T_i) - \min(T_i)}$$

- In the above equation, K is a variable which limits the maximum value of runoff coefficient to K (default=0.8), for roads and concrete surface, which are highly impervious surfaces.
- This parameter K can be slightly calibrated with the help of part of the catchment within the area.
- The equivalent runoff coefficient can be computed by averaging the runoff coefficients of all the pixels.

The results of the image processing were compared with the actual runoff coefficients computed using the Arc-GIS.

4. RESULTS AND DISCUSSION

4.1. Using image processing

4.1.1. Runoff computation for catchment-1

The cropped satellite image along with runoff coefficients and corresponding histograms for the catchment of RWH-1 are shown in Figure 3(a)–3(c), respectively. From the image processing, the area averaged runoff coefficient was found to be 0.2519.

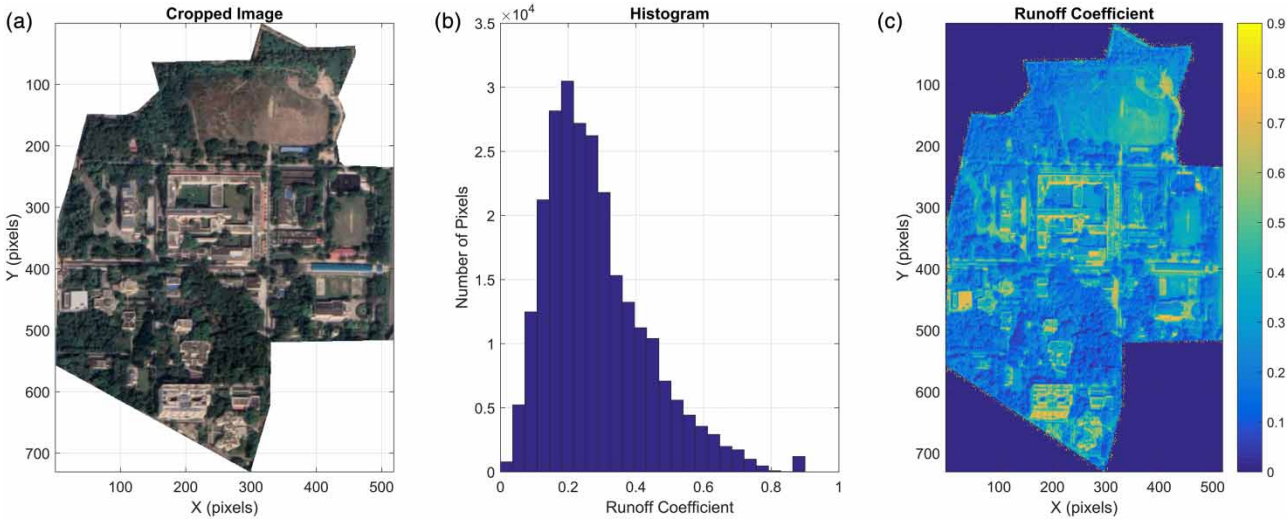

Figure 3 | Catchment for RWH-1: (a) actual cropped satellite image; (b) runoff coefficients; and (c) the histogram of runoff coefficients.

4.1.2. Runoff computation for catchment-2

The cropped satellite image along with runoff coefficients and corresponding histograms for the catchment of RWH-2 are shown in Figure 4(a)–4(c), respectively. From the image processing, the area averaged runoff coefficient was found to be 0.3263.

4.1.3. Runoff computation for catchment-3

The cropped satellite image along with runoff coefficients and corresponding histograms for the catchment of RWH-3 are shown in Figure 5(a)–5(c), respectively. From the image processing, the area averaged runoff coefficient was found to be 0.3554.

4.2. Using Arc-GIS

In the LULC shown in Figure 6, four different types of land types can be seen in the first catchment. The total area of the catchment is 274,991.30 m^2. The maximum percentage of area in the first catchment is covered by forest area. It is

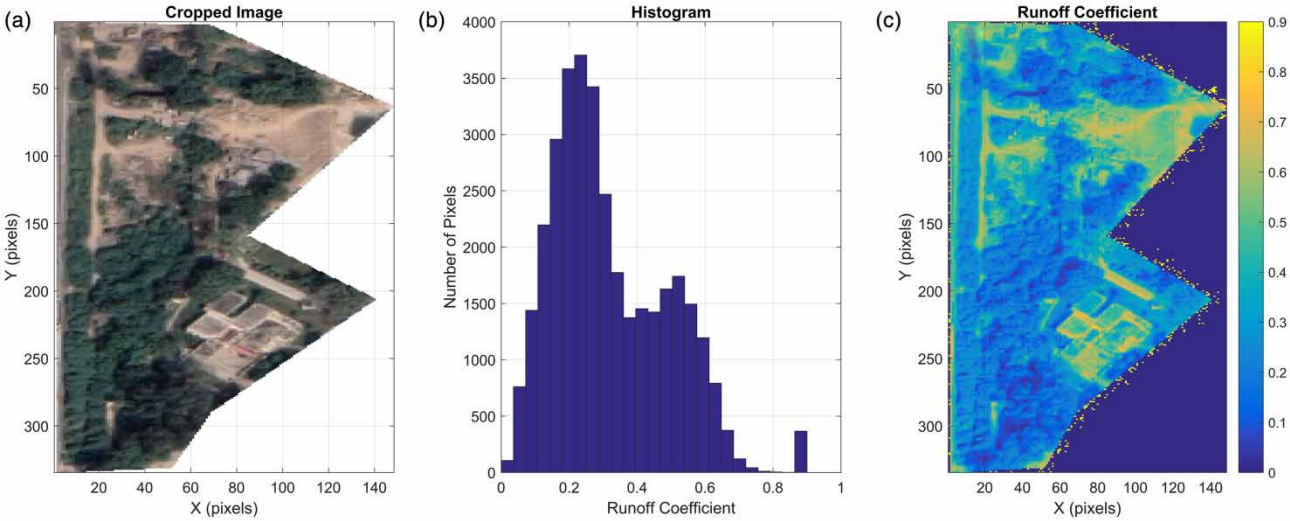

Figure 4 | Catchment for RWH-2: (a) actual cropped satellite image; (b) runoff coefficients; and (c) the histogram of runoff coefficients.

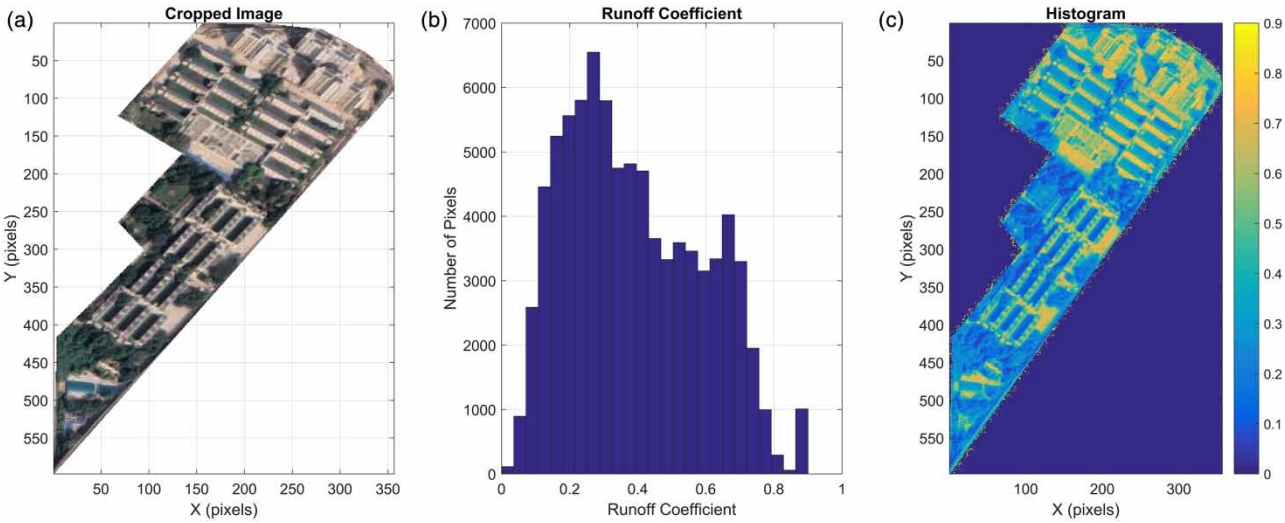

Figure 5 | Catchment for RWH-3: (a) actual cropped satellite image; (b) runoff coefficients; and (c) the histogram of runoff coefficients.

152,911.02 m^2 with a percentage coverage of 55.06% (Table 1). The average runoff coefficient was found to be 0.278. The minimum area coverage was of roads comprising 3.92% of the total area and its runoff coefficient is 0.8. The other two land types are barren lands and commercial areas with percentage coverage of 26.45 and 14.01%, respectively. The commercial area includes the administrative and academic building, residential buildings, and other establishments.

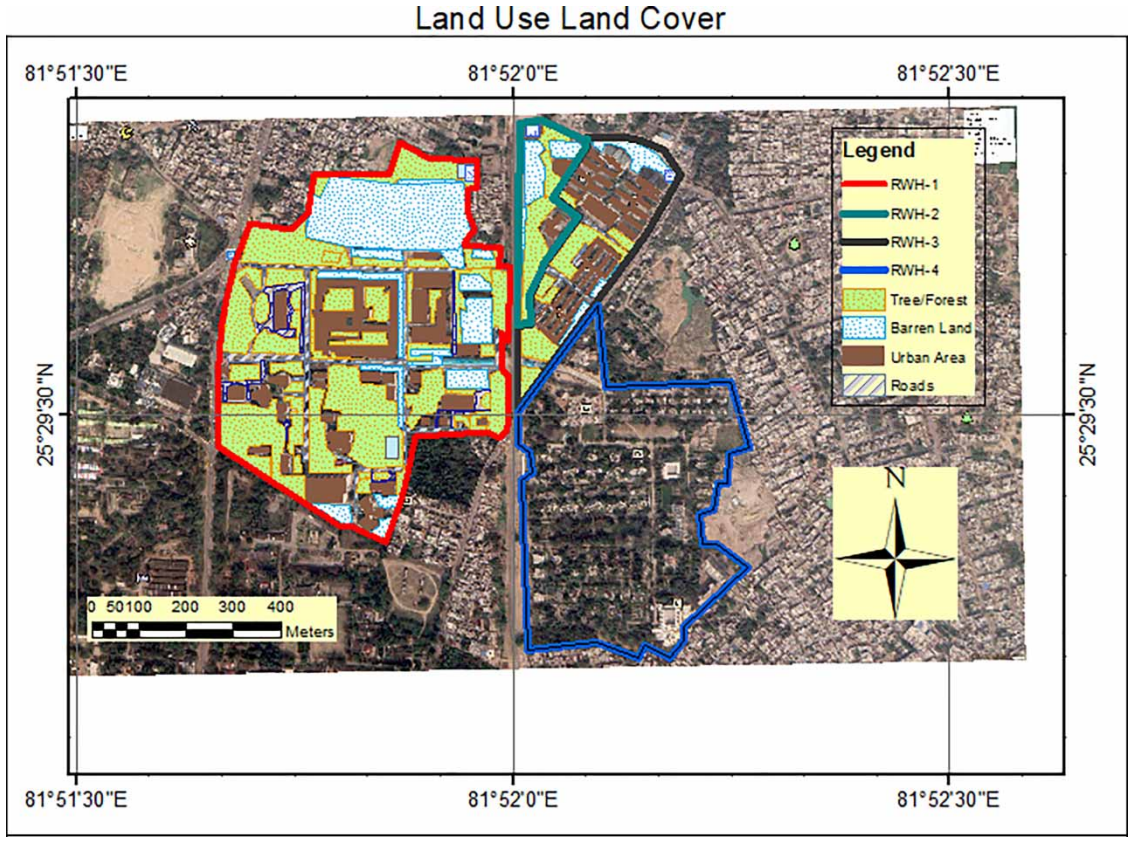

Figure 6 | LULC of the entire study area.

Table 1 | LULC for the RWH-1

SL No	Type of land	C	Area (m^2)	C_{eq}
1	Urban	0.5	38,536.35	
2	Barren lands	0.25	72,743.93	0.278
3	Roads	0.8	10,800	
4	Forest	0.2	152,911	
Total			274,991.3	

Table 2 shows the details of the LULC in the second catchment. The total area of the catchment is 24,170.27 m^2 out of which barren land comprises 56.09% of land cover. The least percentage cover is 9.81% that includes the commercial areas. The forest cover and road coverage are 17.79 and 16.30%, respectively. The equivalent runoff coefficient for the second catchment is obtained as 0.3553.

Finally, the yield is computed for the third catchment. Table 3 shows the percentage of LULC coverage, where the total area is 51,000.63 m^2. In the third catchment, the percentage coverage of the commercial area is 39.99%, which is the maximum, followed by the forest area, which is 31.77% of the catchment area. The percentage coverage of barren land and roads is 14.22 and 14.00%, respectively. The equivalent runoff coefficient using the LULC is obtained as 0.4111 for the third catchment.

4.3. Comparison of both methods

The comparison of the volume of water generated from the two methods is shown in the bar plots below in Table 4. It can be seen that there is less than 10% error in the image processing method by using the default calibration parameter (k=0.8).

Since the error is systematic, we estimated the runoff generated from image processing for k=0.9. The results for the case are shown in Table 5. It can be seen that average error is reduced to near 2% only.

Furthermore, the image processing method is easy and consumes less time in runoff estimation. On average, the time taken for capturing the screenshot, saving it, and running the code takes only less than 1 min for a catchment. However, in the conventional method, proper georeferencing is a crucial step that takes about 5–10 min. Then, marking different types of areas by polygons is also a time-consuming method, taking more than 1 h for the study area. Therefore, the time taken and efforts are significantly reduced in the proposed method without compromising the accuracy.

Table 2 | LULC for the RWH-2

SL No	Type of land	C	Area (m^2)	C_{eq}
1	Urban	0.5	2,371.27	
2	Barren lands	0.25	13,559	0.3553
3	Roads	0.8	3,940	
4	Forest	0.2	4,300	
Total			24,170.27	

Table 3 | LULC for the RWH-3

SL No	Type of land	C	Area (m^2)	C_{eq}
1	Urban	0.5	20,397.99	
2	Barren lands	0.25	7,254.43	0.4111
3	Roads	0.8	7,142.82	
4	Forest	0.2	16,205.39	
Total			51,000.63	

Table 4 | Comparison of both methods for k=0.8

Catchment	Area (m^2)	MATLAB	Arc-GIS	Error (%)
RWH-1	274,991	2,770.8	3,057.89	9.39
RWH-2	24,170	315.46	343.5	8.16
RWH-3	51,000	725.01	838.64	13.55
			Average	9.91

Table 5 | Comparison of both methods for k=0.9

Catchment	Area (m^2)	MATLAB	Arc-GIS	Error (%)
RWH-1	274,991	3,117.29	3,057.89	1.94
RWH-2	24,170	354.89	343.5	3.32
RWH-3	51,000	815.65	838.64	2.74
			Average	2.15

5. SUMMARY AND CONCLUSIONS

In this study, a quantitative comparison has been conducted to investigate the potential of the RWH system in the MNNIT, Allahabad campus in Prayagraj. The campus houses infrastructures like the administrative building, halls, etc., having a large rooftop area that has the potential to collect plenty of rainwater. Thus, the potential of setting an RWH system in the MNNIT campus was studied. Runoff estimation studies in the past are time-intensive as parameter estimation for an area is complex by the conventional method (Arc-GIS). A novel framework is developed to obtain the parameters by simple digital image processing (Google Satellite Image) which were then used to obtain the runoff. This framework is easy and consumes less time in runoff estimation; as the framework can be easily applied to any new area.

The conclusions of the study are as follows:

- The suggested methodology is an easy and fast method as compared to the conventional method for estimating the runoff coefficient for a residential catchment. The residential catchments are defined by the man-made drainage network, hence capturing the residential catchment is easier and can be done without any use of GIS software. However, for the natural catchments, the drainage network is defined based on a digital elevation model, which requires the use of GIS software for the catchment delineation.
- The sum of RGB pixels of the image obtained from Google image was found to be directly correlated with the runoff coefficient for easy calculation.
- Considering the maximum runoff coefficient as nearly 0.9, the default parameter was kept equal to 0.8.
- The entire study area was divided into three catchments. Using the conventional method (Arc-GIS), the equivalent runoff coefficients for these catchments were found to be 0.2780, 0.3553, and 0.4111, respectively. The range of error (compared to conventional method) in runoff obtained from the proposed method with default k value (0.8) were found to be 8.16–13.55% with an average value of 9.91%. However, with slightly modified value of k (0.9), the errors were significantly reduced to 1.94–3.32% with an average of 2.15%.

Thus, it can be concluded that the proposed method is an easy and effective method for quickly computing the runoff for any given residential area for designing RWH system. However, there are certain limitations of this method. The method requires the delineated catchment area and the area must be calculated prior. Furthermore, this method is suitable only for the residential area, not for the natural regions.

DATA AVAILABILITY STATEMENT

Data cannot be made publicly available; readers should contact the corresponding author for details.

CONFLICT OF INTEREST

The authors declare there is no conflict.

REFERENCES

Abdulla, F. A. & Al-Shareef, A. W. 2009 Roof rainwater harvesting systems for household water supply in Jordan. *Desalination* **243** (1–3), 195–207. https://doi.org/10.1016/j.desal.2008.05.013.

Aher, M., Pradhan, S. & Dandawate, Y. 2014 Rainfall estimation over roof-top using land-cover classification of google earth images. In: *2014 International Conference on Electronic Systems, Signal Processing and Computing Technologies*, pp. 111–116.

Al-Ghobari, H. & Dewidar, A. Z. 2021 Integrating GIS-based MCDA techniques and the SCS-CN method for identifying potential zones for rainwater harvesting in a semi-arid area. *Water* **13** (5), 704. https://doi.org/10.3390/w13050704.

Al Qudah, K., Jaradat, R. & Awawdeh, M. 2012 Rainwater harvesting assessment for a small size urban area in Jordan. *International Journal of Water Resources and Environmental Engineering* **4**, 415–412. https://doi.org/10.5897/IJWREE10.025.

Amanatidis, G. T., Paliatsos, A. G., Repapis, C. C. & Bartzis, J. G. 1993 Decreasing precipitation trend in the Marathon area, Greece. *International Journal of Climatology* **13** (2), 191–201. https://doi.org/10.1002/joc.3370130205.

Ammar, A., Riksen, M., Ouessar, M. & Ritsema, C. 2016 Identification of suitable sites for rainwater harvesting structures in arid and semi-arid regions: a review. *International Soil and Water Conservation Research* **4** (2), 108–120. https://doi.org/10.1016/j.iswcr.2016.03.001.

Aung, S. & Thant, H. A. 2019 *LAND COVER INDEX CLASSIFICATION USING SA^{TEL}LITE IMAGES WITH DIFFERENT ENHANCEMENT METHODS*.

Belmeziti, A., Coutard, O. & Gouvello, B. 2014 How much drinking water can be saved by using rainwater harvesting on a large urban area? application to Paris agglomeration. *Water Science and Technology : A Journal of the International Association on Water Pollution Research* **70**, 1782–1788. https://doi.org/10.2166/wst.2014.269.

Biswas, B. K. & Mandal, B. H. 2014 Construction and evaluation of rainwater harvesting system for domestic use in a remote and rural area of Khulna, Bangladesh. *International Scholarly Research Notices* **2014**, e751952. https://doi.org/10.1155/2014/751952.

Eckart, K., McPhee, Z. & Bolisetti, T. 2018 Multiobjective optimization of low impact development stormwater controls. *Journal of Hydrology* **562**, 564–576. https://doi.org/10.1016/j.jhydrol.2018.04.068.

Ekbote, M., Raut, K. & Dandawate, Y. 2017 Determination of area change in water bodies and vegetation for geological applications by using temporal satellite images of IRS 1C/1D. In: *Proceedings of the International Conference on Data Engineering and Communication Technology*. Springer, Singapore, pp. 819–827. https://doi.org/10.1007/978-981-10-1678-3_79.

Falkenmark, M. & Stockholm International Water Institute 2001 *Water Harvesting for Upgrading of Rainfed Agriculture: Problem Analysis and Research Needs*. Stockholm International Water Institute. Available from: http://www.siwi.org/downloads/Reports/Report%2011 %20Water%20Harvesting%20for%20Upgrading2001.pdf.

Farahbakhsh, K., Despins, C. & Leidl, C. 2009 Developing capacity for large-scale rainwater harvesting in Canada. *Water Quality Research Journal* **44** (1), 92–102. https://doi.org/10.2166/wqrj.2009.010.

Fonseca, C. R., Hidalgo, V., Díaz-Delgado, C., Vilchis-Francés, A. Y. & Gallego, I. 2017 Design of optimal tank size for rainwater harvesting systems through use of a web application and geo-referenced rainfall patterns. *Journal of Cleaner Production* **145**, 323–335. https://doi.org/10.1016/j.jclepro.2017.01.057.

Forkuo, E. K. 2013 Using a GIS-based model as a decision support framework for identifying suitable rain water harvesting sites. *International Journal of Advanced Technology & Engineering Research* **3**, 33.

Foster, S. S. D. 1999 Impact of urbanization on groundwater. *IAHS Publn* **198**, 187–207.

Gaikwad, S. 2015 Application of remote sensing and GIS in rainwater harvesting: a case from Goa, India. *International Journal of Scientific and Engineering Research* **6**, 633–639.

Garg, N. K. & Hassan, Q. 2007 Alarming scarcity of water in India. *Current Science* **93** (7), 932–941. http://www.jstor.org/stable/24099258 (Accessed 14 August 2022).

Hafizi Md Lani, N., Yusop, Z. & Syafiuddin, A. 2018 A review of rainwater harvesting in Malaysia: prospects and challenges. *Water* **10** (4), 506. https://doi.org/10.3390/w10040506.

Handia, L., Tembo, J. M. & Mwiindwa, C. 2003 Potential of rainwater harvesting in urban Zambia. *Physics and Chemistry of the Earth, Parts A/B/C* **28** (20), 893–896. https://doi.org/10.1016/j.pce.2003.08.016.

Haque, M. M., Rahman, A. & Samali, B. 2016 Evaluation of climate change impacts on rainwater harvesting. *Journal of Cleaner Production* **137**, 60–69. https://doi.org/10.1016/j.jclepro.2016.07.038.

Hartigan, M. 2009 Help from above: considering rainwater harvesting as an alternative to filtration (*Innovations case discussion*: SONO filters). *Innovations: Technology, Governance, Globalization* **4** (3), 103–106. https://doi.org/10.1162/itgg.2009.4.3.103.

Helmreich, B. & Horn, H. 2009 Opportunities in rainwater harvesting. *Desalination* **248** (1–3), 118–124. https://doi.org/10.1016/j.desal.2008.05.046.

Huang, Z., Nya, E. L., Rahman, M. A., Mwamila, T. B., Cao, V., Gwenzi, W. & Noubactep, C. 2021 Integrated water resource management: rethinking the contribution of rainwater harvesting. *Sustainability* **13** (15), 8338. https://doi.org/10.3390/su13158338.

IFPRI 2012 *Global Hunger Index, Chapter 3: Sustainable Food Security Under Land, Water and Energy Stresses*. International Food Policy Research Institute, Washington DC. Available from: https://www.ifpri.org/publication/2012-global-hunger-index.

Issahaku, A.-R., Campion, B. B. & Edziyie, R. 2016 Rainfall and temperature changes and variability in the upper east region of Ghana: CLIMATE CHANGE AND VARIABILITY. *Earth and Space Science* **3** (8), 284–294. https://doi.org/10.1002/2016EA000161.

Jain, S. K. & Kumar, V. 2012 Trend analysis of rainfall and temperature data for India. *Current Science* **102** (1), 13.

Kemper, K. E. 2004 Groundwater? From development to management. *Hydrogeology Journal* **12** (1), 3–5. https://doi.org/10.1007/s10040-003-0305-1.

Kothyari, U. C. & Singh, V. P. 1996 Rainfall and temperature trends in India. *Hydrological Processes* **10** (3), 357–372. https://doi.org/10.1002/(SICI)1099-1085(199603)10:3<357::AID-HYP305 > 3.0.CO;2-Y.

Lee, K. E., Mokhtar, M., Mohd Hanafiah, M., Abdul Halim, A. & Badusah, J. 2016 Rainwater harvesting as an alternative water resource in Malaysia: potential, policies and development. *Journal of Cleaner Production* **126**, 218–222. https://doi.org/10.1016/j.jclepro.2016.03.060.

Lindh, G. 1983 *Water and the City*. UNESCO, Paris.

Mahmoud, S. H. & Alazba, A. A. 2015 The potential of in situ rainwater harvesting in arid regions: developing a methodology to identify suitable areas using GIS-based decision support system. *Arabian Journal of Geosciences* **8** (7), 5167–5179. https://doi.org/10.1007/s12517-014-1535-3.

Medina, N., Sanchez, A. & Vojinovic, Z. 2012 *Automatic Runoff Coefficient Estimation for Urban Drainage Modeling Using Google Maps Information and Fuzzy Classification*.

Morales-Pinzón, T., Rieradevall, J., Gasol, C. & Gabarrell Durany, X. 2015 Modelling for economic cost and environmental analysis of rainwater harvesting systems. *Journal of Cleaner Production* **87**, 613–626. https://doi.org/10.1016/j.jclepro.2014.10.021.

Norman, M., Shafri, H. Z. M., Mansor, S. B. & Yusuf, B. 2019 Review of remote sensing and geospatial technologies in estimating rooftop rainwater harvesting (RRWH) quality. *International Soil and Water Conservation Research* **7** (3), 266–274. https://doi.org/10.1016/j.iswcr.2019.05.002.

Parker, D. E., Horton, E. B. & Alexander, L. V. 2000 Global and regional climate in 1999. *Weather* **55** (6), 188–199. https://doi.org/10.1002/j.1477-8696.2000.tb04059.x.

Qi, Q., Marwa, J., Mwamila, T. B., Gwenzi, W. & Noubactep, C. 2019 Making rainwater harvesting a key solution for water management: the universality of the Kilimanjaro concept. *Sustainability* **11** (20), 5606. https://doi.org/10.3390/su11205606.

Radzali, N. a. W. M., Shafri, H. Z. M., Norman, M. & Saufi, S. 2018 Roofing assessment for rooftop rainwater harvesting adoption using remote sensing and Gis approach. *The International Archives of the Photogrammetry, Remote Sensing and Spatial Information Sciences* **XLII-4-W9**, 129–132. https://doi.org/10.5194/isprs-archives-XLII-4-W9-129-2018.

Sample, D. J. & Liu, J. 2014 Optimizing rainwater harvesting systems for the dual purposes of water supply and runoff capture. *Journal of Cleaner Production* **75**, 174–194. https://doi.org/10.1016/j.jclepro.2014.03.075.

Sharma, D. & Babel, M. S. 2014 Trends in extreme rainfall and temperature indices in the western Thailand: TRENDS IN WESTERN THAILAND. *International Journal of Climatology* **34** (7), 2393–2407. https://doi.org/10.1002/joc.3846.

Tam, V., Tam, L. & Zeng, S. 2010 Cost effectiveness and tradeoff on the use of rainwater tank: an empirical study in Australian residential decision-making. *Resources, Conservation and Recycling* **54**, 178–186. https://doi.org/10.1016/j.resconrec.2009.07.014.

Thomas, R. B., Kirisits, M. J., Lye, D. J. & Kinney, K. A. 2014 Rainwater harvesting in the United States: a survey of common system practices. *Journal of Cleaner Production* **75**, 166–173. https://doi.org/10.1016/j.jclepro.2014.03.073.

Vieira, A. S., Beal, C. D., Ghisi, E. & Stewart, R. A. 2014 Energy intensity of rainwater harvesting systems: a review. *Renewable and Sustainable Energy Reviews* **34** (C), 225–242.

Wang, X., Jian-yun, Z., Yang, Z., Shahid, S., He, R., Xia, X. & Liu, H. 2013 Historic water consumptions and future management strategies for Haihe River basin of Northern China. *Mitigation and Adaptation Strategies for Global Change* **20**. https://doi.org/10.1007/s11027-013-9496-5.

Ward, S., Memon, F. A. & Butler, D. 2012 Performance of a large building rainwater harvesting system. *Water Research* **46** (16), 5127–5134. https://doi.org/10.1016/j.watres.2012.06.043.

Zabidi, H. A., Goh, H. W., Chang, C. K., Chan, N. W. & Zakaria, N. A. 2020 A review of roof and pond rainwater harvesting systems for water security: the design, performance and way forward. *Water* **12** (11), 3163. https://doi.org/10.3390/w12113163.

Zhou, Y., Shao, W. & Zhang, T. 2010 Analysis of a rainwater harvesting system for domestic water supply in Zhoushan, China. *Journal of Zhejiang University-SCIENCE A* **11** (5), 342–348. https://doi.org/10.1631/jzus.A0900608.

Zhou, X., Bai, Z. & Yang, Y. 2017 Linking trends in urban extreme rainfall to urban flooding in China. *International Journal of Climatology* **37**. https://doi.org/10.1002/joc.5107.

First received 16 May 2022; accepted in revised form 25 July 2022. Available online 10 August 2022